British Journal of Pharmacology

DOI:10.1111/j.1476-5381.2011.01769.x
www.brjpharmacol.org

RESEARCH PAPER

Role of ion channels in sepsis-induced atrial tachyarrhythmias in guinea pigs

Yuta Aoki[1], Noboru Hatakeyama[2], Seiji Yamamoto[3], Hiroyuki Kinoshita[4], Naoyuki Matsuda[5], Yuichi Hattori[3] and Mitsuaki Yamazaki[1]

[1]*Department of Anesthesiology, Graduate School of Medicine and Pharmaceutical Sciences, University of Toyama, Toyama, Japan,* [2]*Department of Anesthesiology, Aichi Medical University, Aichi, Japan,* [3]*Department of Molecular and Medical Pharmacology, Graduate School of Medicine and Pharmaceutical Sciences, University of Toyama, Toyama, Japan,* [4]*Department of Anesthesiology, Wakayama Medical University, Wakayama, Japan, and* [5]*Department of Emergency and Critical Care Medicine, Nagoya University Graduate School of Medicine, Nagoya, Japan*

Correspondence
Dr Y Aoki, Department of Anesthesiology, Graduate School of Medicine and Pharmaceutical Sciences, University of Toyama, Toyama 930-0194, Japan. E-mail: g0049eriki@yahoo.co.jp

Keywords
action potential; atrial myocytes; inducible NOS (iNOS); ion channels; NO; polyphenol; sepsis

Received
28 August 2011
Revised
7 October 2011
Accepted
27 October 2011

BACKGROUND AND PURPOSE

Supraventricular tachyarrhythmias, including atrial fibrillation, are occasionally observed in patients suffering from sepsis. Modulation of cardiac ion channel function and expression by sepsis may have a role in the genesis of tachyarrhythmias.

EXPERIMENTAL APPROACH

Sepsis was induced by LPS (i.p.; 300 μg·kg^{-1}) in guinea pigs. Membrane potentials and ionic currents were measured in atrial myocytes isolated from guinea pigs 10 h after LPS, using whole cell patch-clamp methods.

KEY RESULTS

In atrial cells from LPS-treated animals, action potential duration (APD) was significantly shortened. It was associated with a reduced L-type Ca^{2+} current and an increased delayed rectifier K^+ current. These electrophysiological changes were eliminated when N^G-nitro-L-arginine methyl ester (L-NAME) or *S*-ethylisothiourea was given together with LPS. In atrial tissues from LPS-treated animals, Ca^{2+} channel subunits ($Ca_v1.2$ and $Ca_v1.3$) decreased and delayed rectifier K^+ channel subunits ($K_v11.1$ and $K_v7.1$) increased. However, L-NAME treatment did not substantially reverse such changes in atrial expression in LPS-treated animals, with the exception that $K_v11.1$ subunits returned to control levels. After LPS injection, inducible NOS in atrial tissues was up-regulated, and atrial NO production clearly increased.

CONCLUSIONS AND IMPLICATIONS

In atrial myocytes from guinea pigs with sepsis, APD was significantly shortened. This may reflect nitration of the ion channels which would alter channel functions, rather than changes in atrial expression of the channels. Shortening of APD could serve as one of the mechanisms underlying atrial tachyarrhythmia in sepsis.

Abbreviations

APD, action potential duration; DAF-2 DA, 4,5-diaminofluorescein diacetate; EIT, *S*-ethylisothiourea; eNOS, endothelial NOS; I_{Ca}, inward Ca^{2+} current; ICU, intensive care unit; I_K, delayed rectifier K^+ current; I_{Na}, inward Na^+ current; iNOS, inducible NOS; L-NAME, N^G-nitro-L-arginine methyl ester; LPS, lipopolysaccharide

Introduction

Supraventricular tachyarrhythmias, including atrial fibrillation and flutter, are frequently encountered in surgical and non-surgical intensive care unit (ICU) patients (Artucio and Perrier, 1990). These arrhythmias would result in a longer and more expensive stays in the ICU and in hospital (Ommen *et al.*, 1997; Maisel *et al.*, 2001; Reinelt *et al.*, 2001). Moreover,

their new onset in critically ill patients has been strikingly associated with increased morbidity and mortality (Brathwaite and Weissman, 1998).

Growing evidence suggests that the presence of sepsis is by far the most important risk factor for the development of supraventricular tachyarrhythmias in the ICU. More than three decades ago, Ledingham and McArdle,(1978) found development of atrial fibrillation was not unusual in patients with septic shock. In a retrospective study, sepsis was found to be a significant risk factor associated with new-onset tachyarrhythmias after cardiac surgery (Mayr *et al.*, 2001) and in a prospective case control study performed in a surgical ICU (Knotzer *et al.*, 2000). Furthermore, Bender (1996) showed that 32% of surgical ICU patients who developed supraventricular tachyarrhythmias had an association with sepsis and indicated that the presence of shock, notably septic shock, was an independent risk factor of atrial fibrillation. These clinical reports are consistent with the idea that sepsis is closely associated with the development of new-onset supraventricular tachyarrhythmias and its greater mortality (Goodman *et al.*, 2007).

The mechanisms involved in the occurrence of supraventricular tachyarrhythmias during sepsis remain to be clarified. Generally, the principal mechanisms responsible for tachyarrhythmias are considered to be those of enhanced automaticity, triggered activity or re-entry (Kadish and Passman, 1999). Alterations in structure and function of atrial ion channels associated with the pathophysiology of sepsis may play a role in causing these electrophysiological abnormalities. However, such electrophysiological disturbances in atrial cells under conditions of sepsis are poorly understood.

In the present study, the experiments were undertaken to investigate the changes in function and expression of the membrane ion channels responsible for triggering and maintaining the action potentials in atrial cells from guinea pigs after induction of sepsis with lipopolysaccharide (LPS). During sepsis, inducible NOS (iNOS) can be induced in a variety of cells, including macrophages, vascular smooth muscle cells, cardiac myocytes and endothelial cells, leading to overproduction of NO (Morris and Billiar, 1994). As NO has been shown to modulate a number of cardiac ion channels (Fischmeister *et al.*, 2005; Gonzalez *et al.*, 2009; Tamargo *et al.*, 2010), the regulatory role of excessive NO was also examined in animals treated with the NOS inhibitor N^G-nitro-L-arginine methyl ester (L-NAME) or the selective iNOS inhibitor *S*-ethylisothiourea (EIT).

Methods

Animals and treatments

All animal care and experimental procedures were in accordance with the National Institutes of Health guidelines and were approved by the Animal Use Committee of the University of Toyama. Male Hartley guinea pigs, weighing 200–350 g, were injected with LPS (i.p.; 300 $\mu g \cdot kg^{-1}$; *Escherichia coli* 055; List Biological Laboratories, Campbell, CA) or an equivalent volume of sterile saline, as previously described (Kamiyama *et al.*, 2007). This treatment of guinea pigs with LPS mimicked many of the clinical features of sepsis. Heart rate and respiratory rate were temporally elevated from baseline in the LPS-treated guinea pigs, reaching a maximum at 10 h (from 223 ± 3 to 374 ± 2 beats min^{-1} and from 36 ± 1 to 106 ± 2 min^{-1}, $n = 4$) and declining thereafter. Rectal temperature also showed a peak fall at 10 h after LPS (from 37.4 ± 0.1 to 34.3 ± 0.2°C) and returned to baseline values at 24 h. Furthermore, LPS treatment resulted in a progressive increase in the number of leukocytes from 3820 ± 112 μL^{-1} at 0 h to 10120 ± 199/μL at 10 h remaining high (10620 ± 465 μL^{-1}) at 24 h. These findings prompted us to choose 10 h after LPS as the relevant time point for our measurements. Thus, after 10 h from LPS or saline injection, the animals were killed by an overdose of pentobarbital. In some experiments, i.p. injections of L-NAME (200 $mg \cdot kg^{-1}$) or EIT (5 $mg \cdot kg^{-1}$) were given at the same time as the LPS or saline.

Measurements of action potentials and membrane currents

Single atrial myocytes of the guinea pig were obtained by enzymatic dispersion (Hatakeyama *et al.*, 2002). The hearts were excised and the ascending aorta was cannulated with a dull-edged needle. To wash out the blood, S-MEM solution (Gibco, Carlsbad, CA) containing high Ca^{2+} (1.0 mM) was circulated for 10 min via the coronary artery, and then normal S-MEM solution was circulated for 10 min to remove excessive Ca^{2+}. Subsequently, S-MEM solution containing collagenase (type 1A; 0.02%) and trypsin (0.002%) was circulated for 10 min. The atrial tissue was cut into small pieces in S-MEM solution containing BSA, transferred into KB solution (composition (in mM) 70 glutamic acid, 15 taurine, 30 KCl, 10 KH_2PO_4, 0.5 $MgCl_2$, 11 glucose, 10 HEPES, 0.5 EGTA; pH 7.3), and stored in a refrigerator (5°C) for later use.

Electrophysiological recordings were performed by the whole-cell patch-clamp technique, using glass patch electrodes with a tip diameter 1 μm and a resistance of 3–5 MΩ (Hattori *et al.*, 2000; Hatakeyama *et al.*, 2009). Glass patch electrodes were fabricated with a horizontal microelectrode puller (P-87; Sutter, Novato, CA) from glass microtubes (G-1.5; Narishige, Tokyo, Japan) and heat polished with a microforge (MF-83; Narishige). In order to record membrane currents under whole-cell voltage clamp and action potentials under the current-clamp version of patch clamping, a patch clamp amplifier (EPC-9; Heka, Lambrecht, Germany) was used. Acquisition and analysis of the data were performed by Pulse and Pulsefit software (Heka). The compositions of internal and external solutions were essentially the same as those used in our previous studies (Hatakeyama *et al.*, 2002; 2009). In general, the L-type Ca^{2+} current (I_{Ca}) was elicited by a 200 ms depolarizing test pulse to +10 mV from a holding potential (V_H) of –30 mV in order to avoid the Na^+ current (I_{Na}) and the T-type Ca^{2+} current. We confirmed that this current was completely blocked by the dihydropyridine compound nifedipine at 1 μM. The amplitude of I_{Ca} was thus measured as the difference between the peak of the inward current and the current at the end of the test pulse. Meanwhile, delayed rectifier K^+ current (I_K) was measured; external solution contained 1 μM nifedipine and 100 nM $CaCl_2$ to eliminate the involvement of I_{Ca} in the whole-cell membrane currents. All experiments were carried out at room temperature (21–23°C).

RNA extraction and real-time quantitative PCR

Total RNA was extracted from atrial tissues with the use of an RNeasy Mini Kit (Qiagen, Hilden, Germany) according to the manufacturer's instructions. RNA was reverse-transcribed to cDNA using a PrimeScript RT reagent kit (Takara Bio, Ohtsu, Japan), and PCR was performed with a Takara RNA PCR kit (Takara Bio) as described in the manufacturer's manual. Quantitative PCR assay was performed in 20 μL volumes using optical PCR tubes, and the PCR mixture included SYBR Premix Ex Taq (Takara Bio) and 0.2 pmol·μL^{-1} of each pair of oligonucleotide primers. The reactions were run on an Mx3000P™ Real-Time PCR System (Stratagene, La Jolla, CA). Each experiment was repeated at least twice. The primer pairs were designed for amplifying the following target genomic sequences: $Na_v1.5$ (channel nomenclature follows Alexander *et al.*, 2011) (forward, 5′-CTCCTGCAGCGGCCTAAGAAGCC-3′; reverse, 5′-GCTGTGCTCCCTTCAGAGTAACTGTCCTCG-3′), $Ca_v1.2$ (forward, 5′-GGACACCCGGCCCTCTCCTCG-3′; reverse, 5′-ATGCAAGGGTAGGACTGTC-3′), $K_v11.1$ (forward, 5′-AAGATCCATCGGGATGACCTGCTGG-3′; reverse, 5′-GTTG CCGATTGAAGCCGCCCTC-3′), $K_v7.1$ (forward, 5′-ATCAGG CGCATGCAGTACTTTG-3′; reverse, 5′-TGACATCCCGCACGT CATAAG-3′) and iNOS (forward, 5′-ATGGCCTGCCCCTGGA ATTTCC-3′; reverse, 5′-CTGTAGAGATGACTGGCTTTTCCCA CG-3′). β-Actin (forward, 5′-CATCCGTAAGGACCTCTATG CCAAC-3′; reverse, 5′-ATAGAGCCGCCGATCCACA-3′) was used as a reference gene. Data analysis was carried out with Stratagene software as described by Stratagene.

Western blot analysis

After being removed and rinsed in sterilized PBS on ice, atrial tissues were homogenized in RIPA buffer (Thermo Fisher Scientific, Waltham, MA) and then centrifuged at 600× *g* for 15 min to pellet any insoluble material. When required, the membrane fractions were prepared as described previously (Matsuda *et al.*, 1999; 2006). Thus, the supernatant was then centrifuged at 100 000× *g* for 60 min at 4°C. The membrane pellet was re-suspended in RIPA buffer and saved. Samples (10–20 μg) were run on 7.5% SDS-polyacrylamide gel and electrotransferred to PVDF filter membranes. To reduce non-specific binding, the membrane was blocked for 60 min at room temperature in Odyssey blocking buffer (LI-COR, Lincoln, NE). Thereafter, the membrane was incubated overnight at 4°C with primary antibodies for $Ca_v1.2$ (Millipore, Billerica, MA), $Ca_v1.3$ (Millipore), $K_v11.1$ (Millipore), $K_v7.1$ (Millipore), iNOS (Millipore), endothelial NOS (eNOS; Abcam, Cambridge, UK), α-adaptin (Thermo) and β-actin (Cell Signaling, Danvers, MA) (1:200–1000 dilution) in Odyssey blocking buffer. The membrane was washed six times with PBS with 0.1% Tween 20 and incubated with goat anti-rabbit IRDye 680 or goat anti-mouse IRDye 800 CW (LI-COR) diluted in 1:1500 in Odyssey blocking buffer for 60 min at room temperature. After being washed six times in PBS with 0.1% Tween 20, the blots were visualized using the Odyssey Infrared imaging system from LI-COR.

Imaging of intracellular NO in atrial cells

To detect NO production, we loaded atrial cells with 4,5-diaminofluorescein diacetate (DAF-2 DA; Sekisui Chemical CO., Osaka, Japan). This membrane-permeable dye is hydrolysed intracellularly by cytosolic esterases releasing DAF-2, which is converted in the presence of NO into a fluorescent product, DAF-2 triazole (Kojima *et al.*, 1998; Nakatsubo *et al.*, 1998). The DAF-2 DA was loaded at a concentration of 1 μM in Krebs–Ringer's phosphate (KRP) buffer [composition (mM): 120 NaCl, 4.8 KCl, 0.54 $CaCl_2$, 1.2 $MgSO_4$, 15.9 NaH_2PO_3 and 11 glucose; pH 7.2] in the dark at 37°C for 60 min. The nucleus was counterstained with Hoechst 33258 (Nacalai Tesque, Kyoto, Japan). Immunofluorescence images were traced by means of confocal laser scanning microscopy.

Immunofluorescence and confocal analysis

After atrial tissues had been removed and rinsed in sterilized PBS in ice, the tissues were fixed with 4% buffered formalin solution, immersed in sucrose solution, dipped into OCT compound (Sakura Finetechnical, Tokyo, Japan) and frozen at –20°C. The embedded tissues were sectioned at a thickness of 30 μm and air-dried. For immunofluorescence, rehydrated sections were incubated with the primary antibody, anti-$Na_v1.5$ (Abcam), overnight at 4°C, followed by extensive washes with PBS and incubation with the secondary antibody conjugated to high quality flurophores, Alexa 488 or Alexa 568, overnight at 4°C. Immunofluorescence images were observed under Leica TCS-SP-5 confocal system (Leica, Wetzlar, Germany).

Statistical analysis

Data are expressed as means ± SEM. Statistical assessment of the data was performed using Student's *t*-test or a repeated-measure one-way ANOVA followed by Bonferroni's multiple-comparison test when appropriate. A *P*-value of <0.05 was considered to be statistically significant.

Materials

Pentobarbital was supplied by Abbott Laboratories, Abbott Park, IL and nifedipine, E4031 and Chromanol 29B by Sigma-Aldrich, St. Louis, MO.

Results

Changes in action potentials and membrane currents

When action potentials in atrial myocytes were elicited by current injection at a rate of 2 Hz, action potential duration (APD) was shorter in myocytes from guinea pigs given i.p. injection of 300 μg·kg^{-1} LPS (Figure 1). The APD shortening was more marked at the 30% repolarization level (APD_{30}) than at the 90% repolarization level (APD_{90}). Thus, in the LPS treatment group, APD_{30} and APD_{90} were shortened by 51% and 23% respectively. The resting membrane potential and the maximum rate of rise of action potential (V_{max}) remained unchanged in atrial myocytes from LPS-treated animals. In atrial myocytes from the animals treated with L-NAME co-administered with LPS, APD_{30} and APD_{90} were not significantly different from those of control myocytes. Treatment

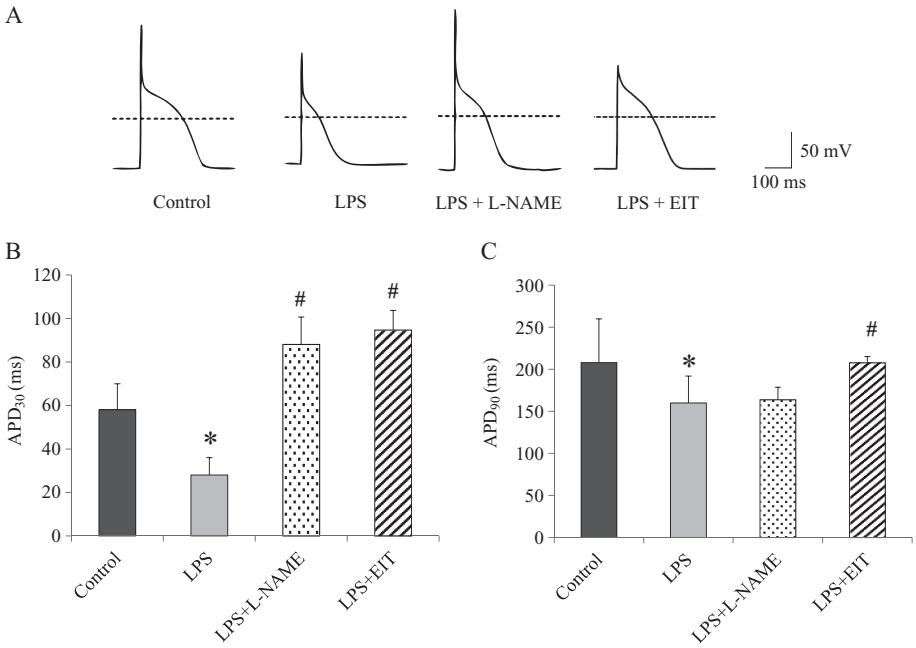

Figure 1

Action potentials in atrial myocytes from control and LPS-challenged guinea pigs. Action potentials were elicited by current injection at a rate of 2 Hz. Animals treated with L-NAME or EIT received i.p. injections of L-NAME or EIT, at the same time as LPS. (A) Typical traces of action potentials are shown. (B, C) Bar graphs comparing APD_{30} and APD_{90} in atrial myocytes from control, LPS-treated, LPS/L-NAME-treated and LPS/EIT-treated animals. Data shown are means ± SEM of 10 cells from at least three different guinea pigs. $^{*}P < 0.05$ significantly different from control. $^{\#}P < 0.05$ significantly different from LPS alone.

with the selective iNOS inhibitor EIT also significantly reversed the APD shortening seen in myocytes from LPS-treated animals.

In each voltage-clamp experiment, membrane capacitance was measured immediately after disruption of the membrane patch. Membrane capacitance of atrial myocytes from LPS-treated animals (25.1 ± 2.2 pF, $n = 20$) did not differ from that of controls (30.9 ± 1.9 pF, $n = 20$). Typical tracings of I_{Ca} elicited by a depolarizing pulse from a holding potential of −30 to +10 mV in atrial myocytes from control, LPS-treated, LPS/L-NAME-treated and LPS/EIT-treated animals are shown in Figure 2A. The net I_{Ca} obtained in myocytes from LPS-treated animals was much smaller than in controls (Figure 2B). The estimated density of I_{Ca} was significantly greater in myocytes from control animals (4.69 ± 0.48 pA/pF) than those from LPS-treated animals (2.24 ± 0.32 pA/pF, $n = 10$ for each group).

The addition of 100 nM isoprenaline resulted in a large increase in I_{Ca} in control myocytes (2.7-fold), which was less pronounced in the LPS-treated group (2.1-fold; Figure 2A,B). As illustrated in Figure 2C, the current–voltage relationships showed that isoprenaline produced a larger increase in I_{Ca} at each test pulse in control myocytes than in those from LPS-treated animals. Treatment with L-NAME or EIT had no effect on the response to isoprenaline on I_{Ca} in the control group but significantly normalized basal and isoprenaline-stimulated I_{Ca} in the LPS-treated group (Figure 2).

Typical tracings of I_K elicited by a 2 s depolarizing pulse from a holding membrane potential of −30 to +60 mV in atrial myocytes from control, LPS-treated, LPS/L-NAME-treated and LPS/EIT-treated animals are shown in Figure 3A. The activating current of I_K was clearly larger in the LPS-treated group than in the control group. The current–voltage relationships in 10 different cells for each group showed that the outward current at each test pulse was significantly increased in the LPS-treated group compared with the control group (Figure 3B). The increase in I_K was not observed in myocytes from the animals when L-NAME or EIT was given together with LPS (Figure 3).

After the rapid component of I_K (I_{Kr}) was blocked by its specific blocker E-4031 (5 μM), the residual major part of the current was eliminated by further administration of 30 μM chromanol 293B, an inhibitor of the slow component of I_K (I_{Ks}) in both atrial myocytes from control and LPS-treated animals (Figure 4A). Conversely, in the presence of chromanol 293B, further addition of E-4031 had little effect on the activating current of I_K in the two different myocytes (Figure 4B). These observations are indicative of a predominant increase in I_{Ks} in atrial myocytes from LPS-treated animals.

Changes in atrial expression of channel subunits

$Ca_v1.2$ and $Ca_v1.3$ phenotypes encode dihydropyridine-sensitive L-type Ca^{2+} channels in atrial myocytes (Zhang *et al.*, 2005), but the dominant high-voltage activated Ca^{2+} channels are $Ca_v1.2$ (Bohn *et al.*, 2000). Western blot analysis showed significantly lowered expression of $Ca_v1.2$ (Figure 5A) and $Ca_v1.3$ (data not shown) protein in atrial tissues from LPS-treated guinea pigs. L-NAME treatment did not signifi-

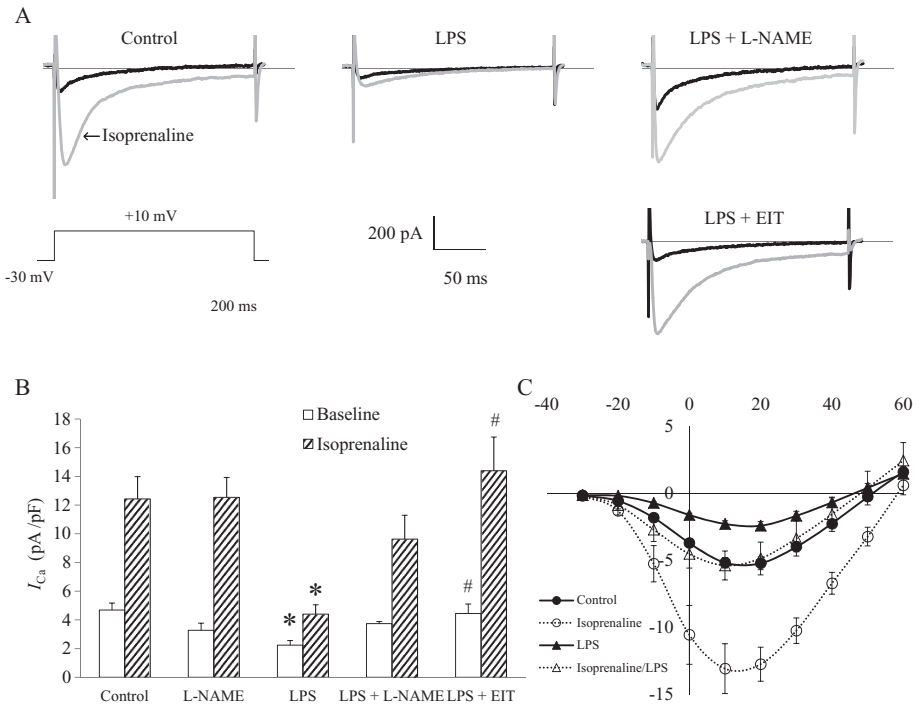

Figure 2

Basal and isoprenaline-stimulated I_{Ca} in atrial myocytes from control and LPS-challenged guinea pigs with and without L-NAME or EIT treatment. (A) Current traces before and 5 min after exposure to 100 nM isoprenaline are superimposed. I_{Ca} was elicited by a 200 ms depolarizing test pulse to +10 mV from a holding potential of 30 mV. (B) Bar graph comparing basal and isoprenaline-stimulated I_{Ca} elicited by a depolarizing pulse from 30 to +10 mV in atrial myocytes from control, L-NAME-treated, LPS-treated and LPS/L-NAME-treated animals. *$P < 0.05$ significantly different from control. $^{\#}P < 0.05$ significantly different from LPS alone. (C) Current–voltage relations for control and septic atrial myocytes before and after exposure to 100 nM isoprenaline. There were significant differences between control and septic current–voltage relation curves in both the absence and presence of isoprenaline ($P < 0.05$). Data shown are means ± SEM of 10 cells from at least three different guinea pigs.

cantly affect the changes in protein levels of $Ca_v1.2$ and $Ca_v1.3$ in atrial tissues from LPS-treated animals. Quantitative real-time PCR revealed that $Ca_v1.2$ mRNA was less abundantly expressed in atrial tissues from LPS-treated animals compared with controls (Figure 5B). This reduced expression of $Ca_v1.2$ mRNA was unaffected by L-NAME, given together with LPS.

The $K_v11.1$ subunit is the principal component of the rapid delayed rectifier K^+ channel, while $K_v7.1$ forms the slow component of the delayed rectifier K^+ channel (Mitcheson and Sanguinetti, 1999; Sanguinetti, 2010). When we determined $K_v11.1$ and $K_v7.1$ protein expression in atrial tissues by Western blotting, induction of sepsis by LPS moderately, but significantly, increased these K^+ channel proteins (Figure 6A). L-NAME treatment did not alter $K_v11.1$ protein expression but resulted in a significant return of $K_v7.1$ protein expression to control levels in atrial tissues from LPS-treated animals. In contrast to protein expression, the mRNA expression levels of $K_v11.1$ and $K_v7.1$ remained substantially unchanged in atrial tissues from LPS-injected guinea pigs regardless of whether L-NAME was co-administered (Figure 6B).

We also assessed mRNA and protein expression of the cardiac Na^+ channel isoform $Na_v1.5$ in atrial tissues using real-time PCR and immunofluorescence assay respectively. No significant difference was observed between the control and LPS-treated groups (data not shown).

Changes in iNOS and eNOS expression and NO production

On Western blots, atrial tissues from control guinea pigs showed a low level of 130 kDa iNOS protein, which doubled in those from LPS-treated animals (Figure 7A). Higher expression of iNOS in atrial tissues from LPS-treated animals was also found at the mRNA level (Figure 7B). No significant difference in atrial eNOS expression levels was found between the control and LPS-treated groups (Figure 7C).

We assessed whether NO production actually increases in atrial cells from LPS-treated guinea pigs, using the fluorescent dye DAF-2 DA (Figure 8). A strong intensity of staining was observed in atrial cells from LPS-treated animals. When L-NAME or EIT was given together with LPS, the intensity of staining declined to the control level.

Discussion

Earlier studies reported a significant reduction in I_{Ca} in ventricular myocytes isolated from LPS-injected guinea pigs and

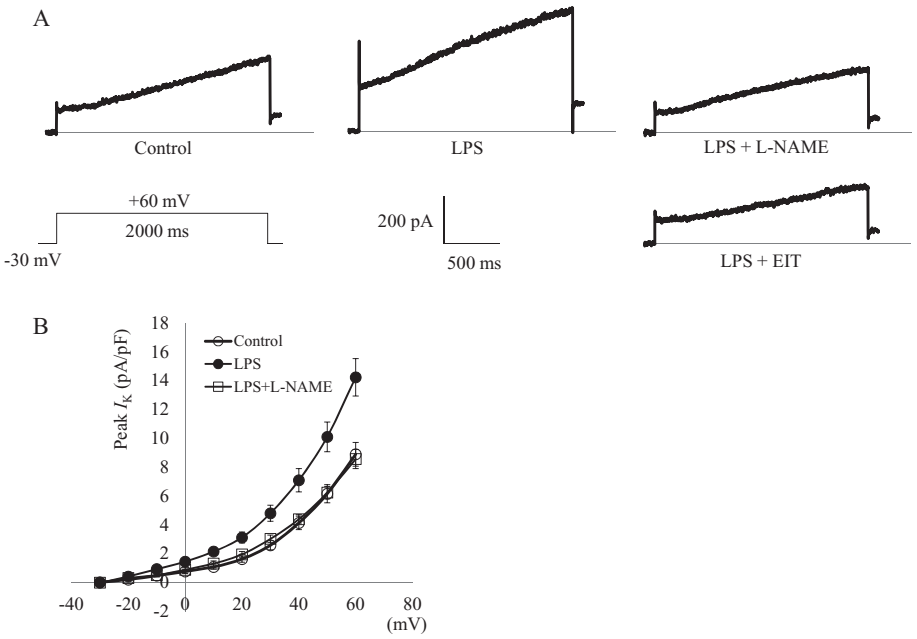

Figure 3

Effect of treatment with L-NAME or EIT on the change in I_K in atrial myocytes from LPS-challenged guinea pigs. (A) Typical tracings of I_K elicited by a 2 s depolarizing test pulse to +60 mV from a holding potential of 30 mV. (B) Current–voltage relations in atrial myocytes from control, LPS-treated and LPS/L-NAME-treated animals. In this current–voltage relation curves, significant differences were found between control and LPS-treated animals ($P < 0.05$), and also between LPS-treated and LPS/L-NAME-treated animals ($P < 0.05$). Data shown are means ± SEM of 10 cells from at least three different guinea pigs.

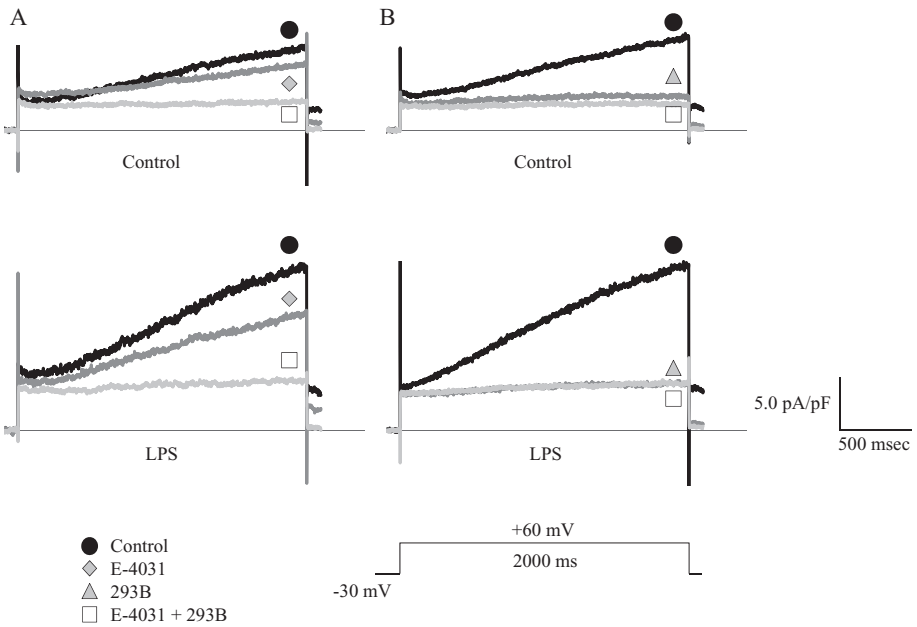

Figure 4

Changes in I_K in the presence of the I_{Kr} inhibitor E-4031 and/or the I_{Ks} inhibitor chromanol 293B in atrial myocytes from control and LPS-challenged guinea pigs. (A) Cells were initially given 5 μM E-4031 followed by 30 μM chromanol 293B. (B) Cells were initially given 30 μM chromanol 293B followed by 5 μM E-4031.

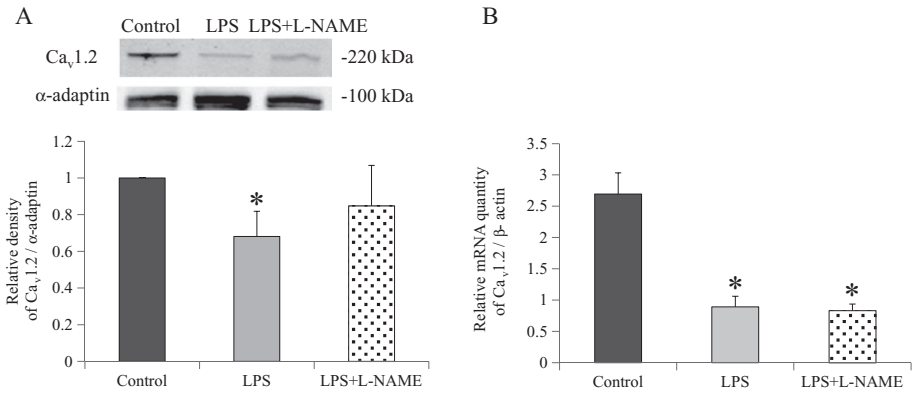

Figure 5

Changes in atrial expression of the Ca^{2+} channel subunit $Ca_v1.2$ in LPS-challenged guinea pigs. (A) Atrial expression of $Ca_v1.2$ protein levels in control and LPS-challenged guinea pigs was compared with the relative level using the endocytic protein α-adaptin. Typical Western blots of $Ca_v1.2$ and α-adaptin are shown in the top trace. Data shown are means ± SEM of four separate experiments. *$P < 0.05$ significantly different from control. (B) Real-time PCR analysis of $Ca_v1.2$ mRNA expression in atrial tissues from control, LPS-treated, and LPS/L-NAME-treated animals. The $Ca_v1.2$ mRNA levels are normalized to β-actin mRNA levels. Data shown are means ± SEM of six separate experiments. *$P < 0.05$ significantly different from control.

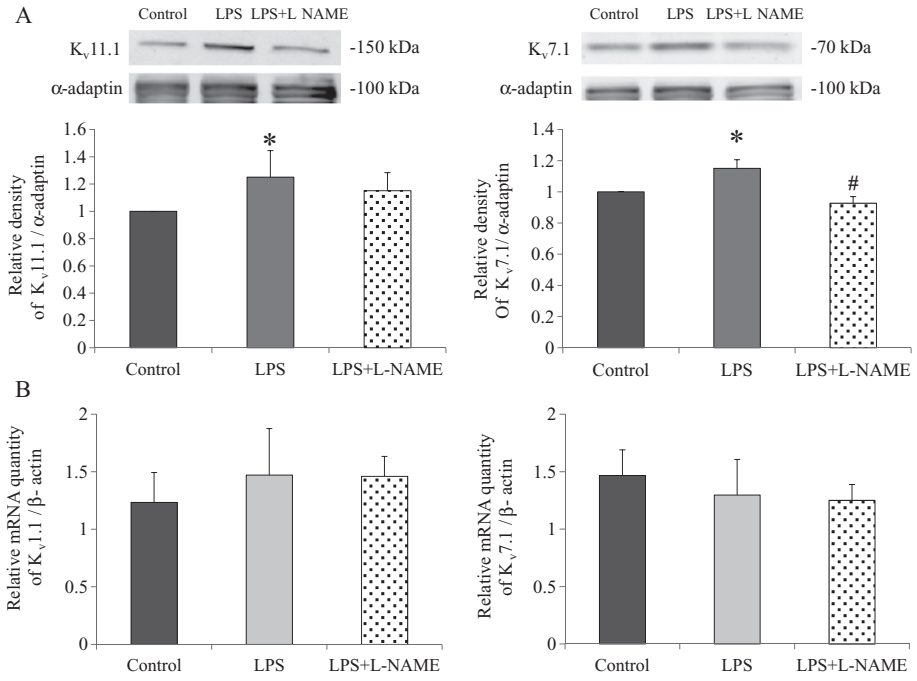

Figure 6

Changes in atrial expression of delayed rectifier K^+ channel subunits ($K_v11.1$ and $K_v7.1$) in LPS-challenged guinea pigs. (A) Atrial expression of delayed rectifier K^+ channel subunit protein levels in control and LPS-challenged guinea pigs was compared with the endocytic protein α-adaptin. Typical Western blots of $K_v11.1$, $K_v7.1$, and α-adaptin are shown in the top trace. Data shown are means ± SEM of six separate experiments. *$P < 0.05$ significantly different from control. $^{\#}P < 0.05$ significantly different from LPS alone. (B) Real-time PCR analysis of delayed rectifier K^+ channel subunit mRNA expression in atrial tissues from control, LPS-treated and LPS/L-NAME-treated guinea pigs. The delayed rectifier K^+ channel subunit mRNA levels are normalized to β-actin mRNA levels. Data shown are means ± SEM of six separate experiments. No significant differences in the atrial expression of delayed rectifier K^+ channel subunit mRNA among groups was noted.

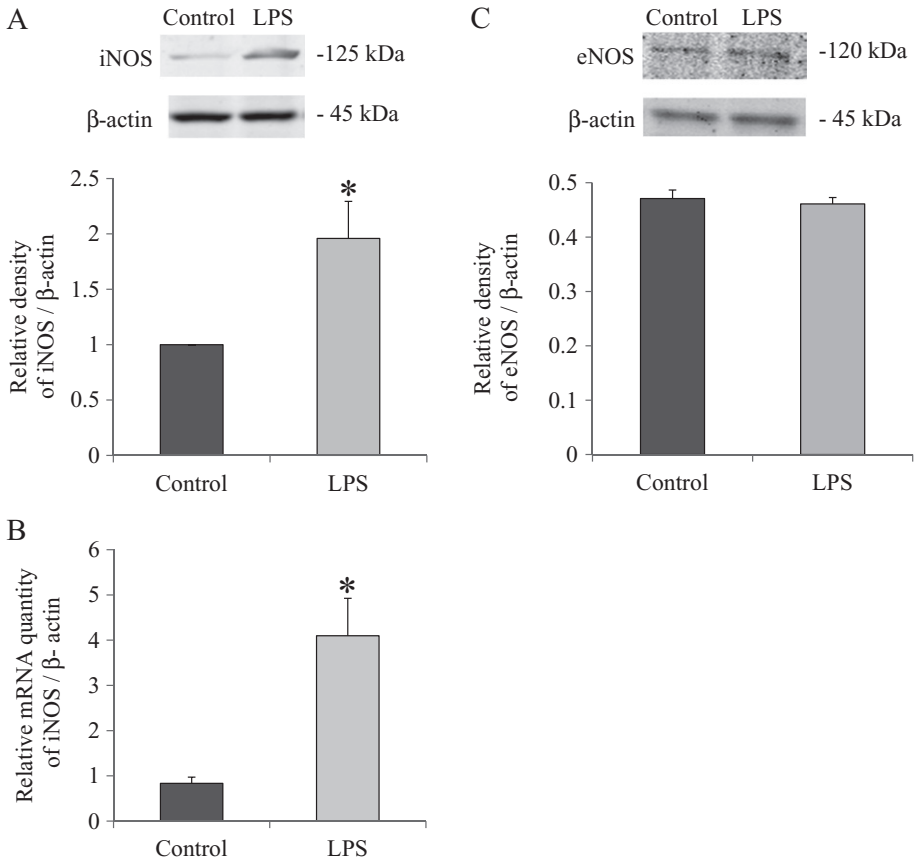

Figure 7

Changes in atrial expression of iNOS and eNOS in LPS-challenged guinea pigs. (A) Atrial expression of iNOS protein levels in control and LPS-challenged guinea pigs was compared with the housekeeping protein β-actin. Typical Western blots of iNOS and β-actin are shown in the top trace. Data shown are means ± SEM of three separate experiments. *$P < 0.05$ significantly different from control. (B) Real-time PCR analysis of iNOS mRNA expression in atrial tissues from control and LPS-challenged guinea pigs. The iNOS mRNA levels are normalized to β-actin mRNA levels. Data shown are means ± SEM of six separate experiments. *$P < 0.05$ significantly different from control. (C) Atrial expression of eNOS protein levels in control and LPS-challenged guinea pigs was compared with β-actin. Typical Western blots of eNOS and β-actin are shown in the top trace. Data shown are means ± SEM of four separate experiments.

rats (Zhong *et al.*, 1997; Abi-Gerges *et al.*, 1999). Thus, *in vivo* administration of LPS has been shown to result in reduced Ca^{2+} influx through L-type Ca^{2+} channels in isolated ventricular myocytes. Although whole-cell voltage-clamp experiments may have technical limitations inherent to measurement of I_{Ca}, we revealed a considerable reduction in I_{Ca} in atrial myocytes isolated from LPS-injected guinea pigs. This was clear in our assays of I_{Ca} elicited by a depolarizing pulse from −30 to +10 mV. A reduction in I_{Ca} of atrial myocytes from LPS-treated guinea pigs did not result from alterations in the voltage-dependent properties of the L-type Ca^{2+} channel, because currents of both atrial myocytes from control and LPS-treated animals had similar voltage dependence, as indicated by the similar current–voltage relationships. Abnormal temperature, heart rate, respiratory rate and white blood cell count observed in LPS-treated guinea pigs suggest that this animal model fulfils several criteria of clinical sepsis. Therefore, the host response to sepsis involved a reduction in I_{Ca} of atrial myocytes.

In sepsis, pro-inflammatory stimuli lead to overexpression of iNOS in many organs. Excessive NO generated by iNOS is implicated in the pathophysiology of sepsis (Titheradge, 1999). In this study, we also observed a significant increment of gene and protein expression of iNOS and a clear overproduction of NO in atrial cells from our animal model of sepsis. Importantly, when L-NAME or EIT was given together with LPS to inhibit iNOS activity, the reduction in I_{Ca} of atrial myocytes was abolished. Recent studies suggest that reactive nitrogen species, including NO, peroxynitrite ($ONOO^-$) and nitrogen dioxide (NO_2), can modulate ion channel structure and function (Matalon *et al.*, 2003). These reactive nitrogen species are known to mediate protein tyrosine nitration (Radi, 2004). Indeed, our immunofluorescence study showed that sections from LPS-induced septic guinea pigs exhibited significant immunostaining with the polyclonal antibody to nitrotyrosine (unpublished observations). Inflammatory colitis results in the nitration of Y^{1837} and Y^{2134} within the C-terminus of human smooth muscle Ca^{2+} channel, $Ca_v1.2b$, and thereby impairs the ability of the tyrosine kinase, c-src kinase, to phosphorylate the Ca^{2+} channel, leading to diminished Ca^{2+} current and muscle contraction during colonic inflammation (Ross *et al.*, 2007). We

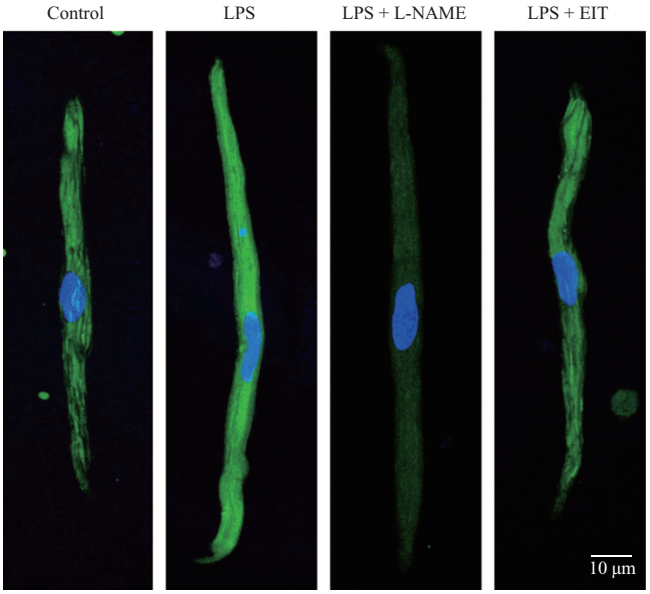

Figure 8

NO production by atrial cells from control and LPS-challenged guinea pigs. When the animals were treated with L-NAME or EIT, i.p. injection of L-NAME or EIT was given together with LPS. Intracellular NO is visualized with the use of the NO-sensitive dye DAF-2 DA (green). Nuclei were stained with Hoechst 33258 (blue). Representative images from two separate experiments are shown.

thus assume that iNOS-induced over-productive NO during sepsis may act as a means of increasing tyrosine nitration of L-type Ca^{2+} channels in atrial myocytes, leading to impaired function of the channels. Interestingly, the $Ca_v1.2$ subunit of the L-type Ca^{2+} channel was hypernitrosylated in left atrial tissues from patients with atrial fibrillation (Carnes *et al.*, 2007).

In atrial myocytes from septic guinea pigs, the APD was significantly shortened, without changes in the resting membrane potential and the maximum rate of rise of action potential. Similar to its effect on I_{Ca}, L-NAME or EIT treatment abolished the APD shortening seen in atrial myocytes from septic animals. This suggests that the shortening of APD was associated with the iNOS-mediated increases in NO. Alternatively, the sepsis-related atrial APD shortening might have arisen from a reduction in I_{Ca} due to tyrosine nitration of L-type Ca^{2+} channels. A decrease in I_{Ca}, which shortens the APD, is one of electrophysiological alterations associated with the genesis of atrial tachyarrhythmias, including atrial fibrillation (Skasa *et al.*, 2001; Van Wagoner, 2008).

The present study showed that the increasing effect of β-adrenoceptor stimulation on I_{Ca} was markedly depressed in atrial myocytes from septic animals. This finding is in marked contrast with a previous report that β-adrenoceptor stimulation reversed the reduction in I_{Ca} in ventricular myocytes 4 h after LPS injection (Zhong *et al.*, 1997). However, the β-adrenoceptor control of I_{Ca} may be modified in a time-dependent manner after LPS challenge. Abi-Gerges *et al.* (1999) found that the decrease of I_{Ca} in ventricular myocytes from LPS-treated rat was compensated by an early potentiation of the β-adrenoceptor response, but this stimulatory effect on I_{Ca} declined at the late stage of sepsis. In other words, the regulatory influence of sepsis on the β-adrenoceptor response on I_{Ca} may be different between atrial and ventricular myocytes. When L-NAME or EIT was co-administered with LPS, the I_{Ca} response to β-adrenoceptor stimulation in atrial myocytes was nearly normalized, suggesting that tyrosine nitration can markedly affect β-adrenoceptor-mediated, L-type Ca^{2+} channel function in atrial myocytes.

L-type Ca^{2+} channels are heteromultimeric complexes of a pore-forming, transmembrane-spanning α_1-subunit, a disulphide-linked complex of α_2- and δ-subunits and an intracellular β- and γ-subunits (Catterall, 1995; Walker and De Waard, 1998). The α_1-subunit is the largest and incorporates the conduction pore, the voltage sensor, gating apparatus and the known sites of channel regulation by second messengers, drugs and toxins. Previous data suggest that cardiac tissues express mainly L-type Ca^{2+} channels containing the α_{1C} subunit ($Ca_v1.2$), but those containing the α_{1D} subunit ($Ca_v1.3$) are found in atrial tissues (Bohn *et al.*, 2000; Zhang *et al.*, 2005). In this study, we found that both $Ca_v1.2$ and $Ca_v1.3$ subunit expression were significantly down-regulated in atrial tissues after sepsis. However, this is likely to be independent of iNOS-related changes, because L-NAME treatment did not substantially reverse the changes in protein levels of $Ca_v1.2$ and $Ca_v1.3$ in atrial tissues from septic animals. In light of the fact that the sepsis-induced reduction in atrial I_{Ca} was prevented by L-NAME treatment, down-regulation of α_1 subunits did not appear to contribute to the reduced I_{Ca} in atrial myocytes from septic animals.

In addition to the change in I_{Ca}, atrial myocytes from septic guinea pigs exhibited a significant increase in I_K. Since I_K is one of the major components that determine the timing of repolarization of cardiomyocytes, the increase in I_K could also contribute to the shortening of APD in atrial myocytes from septic guinea pigs. Treatment with L-NAME reversed the I_K increase seen in atrial myocytes from septic animals, implying involvement of iNOS-mediated over-production of NO in this electrophysiological change. It has been reported that nitrosylation increases I_{Ks} in a manner dependent on eNOS in guinea pig ventricular myocytes, resulting in a shortening of the APD (Bai *et al.*, 2004; 2005). Furthermore, over-expression of CAPON (carboxy-terminal PDZ ligand of neuronal NOS), a binding protein for neuronal NOS, has been demonstrated to result in increased I_{Ks} and shortened APD in guinea pig ventricular myocytes (Chang *et al.*, 2008). Our experiments, with the use of E-4031 and chromanol 293B, which selectively block I_{Kr} and I_{Ks}, respectively, suggest a predominant increase in I_{Ks} in atrial myocytes from septic guinea pigs. We observed that protein expression of $K_v11.1$ and $K_v7.1$, which underlie the rapid component and the slow component of the delayed rectifier K^+ channel, respectively (Mitcheson and Sanguinetti, 1999; Sanguinetti, 2010), were increased in atrial tissues from septic animals. Interestingly, L-NAME treatment resulted in a significant return of protein expression of $K_v7.1$, which forms the slow component of the delayed rectifier K^+ channel, to control levels in atrial tissues from septic animals However, the sepsis-induced increase in protein expression of $K_v11.1$ and $K_v7.1$ was significant but not striking, and their gene expression remained substantially unchanged in sepsis, regardless of treatment with L-NAME.

In conclusion, the data presented here indicate that atrial myocytes from septic guinea pigs display a shortening of the APD, resulting from a decrease in I_{Ca} and an increase in I_K. These electrophysiological alterations appeared to be attributable to the nitration of the ion channels rather than to changes in atrial expression of the ion channels. Given the importance of APD shortening in the induction of arrhythmias, the present results may be relevant to understanding the mechanisms responsible for the occurrence of atrial tachyarrhythmias, including atrial fibrillation, in sepsis.

Acknowledgements

This work was supported in part by a Grant-in-Aid for Scientific Research from the Ministry of Education, Culture, Sports, Science and Technology of Japan. We thank Toshio Fujimori for his excellent technical assistance.

Conflict of interest

All of the authors have no conflict of interest on this manuscript.

References

Abi-Gerges N, Tavernier B, Mebazaa A, Faivre V, Paqueron X, Payen D *et al.* (1999). Sequential changes in autonomic regulation of cardiac myocytes after *in vivo* endotoxin injection in rat. Am J Respir Crit Care Med 160: 1196–1204.

Alexander SPH, Mathie A, Peters JA (2011). Guide to Receptors and Channels (GRAC), 5th Edition. Br J Pharmacol 164 (Suppl. 1): S1–S324.

Artucio H, Perrier M (1990). Cardiac arrhythmias in critically ill patients: epidemiologic study. Crit Care Med 18: 1383–1388.

Bai C-X, Takahashi K, Masumiya H, Sawanobori T, Furukawa T (2004). Nitric oxide-dependent modulation of the delayed rectifier K^+ current and the L-type Ca^{2+} current by ginsenoside Re, an ingredient of *Panax* ginseng, in guinea-pig cardiomyocytes. Br J Pharmacol 142: 567–575.

Bai C-X, Namekata I, Kurokawa J, Tanaka H, Shigenobu K, Furukawa T (2005). Role of nitric oxide in Ca^{2+} sensitivity of the slowly activating delayed rectifier K^+ current in cardiac myocytes. Circ Res 96: 64–72.

Bender JS (1996). Supraventricular tachyarrhythmias in the surgical intensive care unit: an under-recognized event. Ann Surg 62: 73–75.

Bohn G, Moosmang S, Conrad H, Ludwig A, Hofmann F, Klugbauer N (2000). Expression of T- and L-type calcium channel mRNA in murine sinoatrial node. FEBS Lett 481: 73–76.

Brathwaite D, Weissman C (1998). The new-onset of atrial arrhythmias following major noncardiothracic surgery is associated with increased mortality. Chest 114: 462–468.

Carnes CA, Janssen PL, Ruehr ML, Nakayama H, Nakayama T, Haase H *et al.* (2007). Atrial glutathione content, calcium current, and contractility. J Biol Chem 282: 28063–28073.

Catterall WA (1995). Structure and function of voltage-gated ion channels. Annu Rev Biochem 64: 493–531.

Chang K-C, Barth AS, Sasano T, Kizana E, Kashiwakura Y, Zhang Y *et al.* (2008). CAPON modulates cardiac repolarization via neuronal nitric oxide synthase signaling in the heart. Proc Natl Acad Sci U S A 105: 4477–4482.

Fischmeister R, Castro L, Abi-Gerges A, Rochais E, Vandecasteele G (2005). Species- and tissue-dependent effects of NO and cyclic GMP on cardiac ion channels. Comp Biochem Physiol A Mol Integr Physiol 142: 136–143.

Gonzalez DR, Treuer A, Sun QA, Stamler JS, Hare JM (2009). S-Nitrosylation of cardiac ion channels. J Cardiovasc Pharmacol 54: 188–195.

Goodman S, Shirov T, Weissman C (2007). Supraventricular arrhythmias in intensive care unit patients: short and long-term consequences. Anesth Analg 104: 880–886.

Hatakeyama N, Yamada M, Shibuya N, Yamazaki M, Yamamura S, Sugaya M *et al.* (2002). Effects of ropivacaine on membrane potential and voltage-dependent calcium channel current in single guinea-pig ventricular myocytes. J Anesth 16: 273–278.

Hatakeyama N, Sakuraya F, Matsuda N, Kimura J, Kinoshita H, Kemmotsu O *et al.* (2009). Pharmacological significance of the blocking action of the intravenous general anesthesia propofol on the slow component of cardiac delayed rectifier K^+ current. J Pharmacol Sci 110: 334–343.

Hattori Y, Matsuda N, Kimura J, Ishitani T, Tamada A, Gando S *et al.* (2000). Diminished function and expression of the cardiac Na^+-Ca^{2+} exchanger in diabetic rats: implication in Ca^{2+} overload. J Physiol 527: 85–94.

Kadish A, Passman R (1999). Mechanisms and management of paroxysmal supraventricular tachycardia. Cardiol Rev 7: 254–264.

Kamiyama K, Matsuda N, Yamamoto S, Takano K, Takano Y, Yamazaki H *et al.* (2007). Modulation of glucocorticoid receptor expression, inflammation, and cell apoptosis in septic guinea pigs using methylprednisolone. Am J Physiol Lung Cell Mol Physiol 295: L998–L1006.

Knotzer H, Mayr A, Ulmer H, Lederer W, Schobersberger W, Mutz N *et al.* (2000). Tachyarrhythmias in a surgical intensive care unit: a case-controlled epidemiologic study. Intensive Care Med 26: 908–914.

Kojima H, Nakatsubo N, Kikuchi K, Kawahara S, Kirino Y, Nagoshi H *et al.* (1998). Detection and imaging of nitric oxide with novel fluorescent indicators: diaminofluoresceins. Anal Chem 70: 2446–2453.

Ledingham IM, McArdle CS (1978). Prospective study of the treatment of septic shock. Lancet 1: 1194–1197.

Maisel WH, Rawn JD, Stevenson WG (2001). Atrial fibrillation after cardiac surgery. Ann Intern Med 135: 1061–1073.

Matalon S, Hardiman KM, Jain L, Eaton DC, Kotlikoff M, Eu JP *et al.* (2003). Regulation of ion channel structure and function by reactive oxygen-nitrogen species. Am J Physiol Lung Cell Mol Physiol 285: L1184–L1189.

Matsuda N, Hattori Y, Gando S, Akaishi Y, Kemmotsu O, Kanno M (1999). Diabetes-induced down-regulation of β_1-adrenoceptor mRNA expression in rat heart. Biochem Pharmacol 58: 881–885.

Matsuda N, Hayashi Y, Takahashi Y, Hattori Y (2006). Phosphorylation of endothelial nitric-oxide synthase is diminished in mesenteric arteries from septic rabbits depending on the altered

phosphatidylinositol 3-kinase/Akt pathway: reversal effect of fluvastatin therapy. J Pharmacol Exp Ther 319: 1348–1354.

Mayr A, Knotzer H, Pajk W, Luckner G, Ritsch N, Dünser M *et al*. (2001). Risk factors associated with new onset tachyarrhythmias after cardiac surgery – a retrospective analysis. Acta Anaesthesiol Scand 45: 543–549.

Mitcheson JS, Sanguinetti MC (1999). Biophysical properties and molecular basis of cardiac rapid and slow delayed rectifier potassium channels. Cell Physiol Biochem 9: 201–216.

Morris SM Jr, Billiar TR (1994). New insights into the regulation of inducible nitric oxide synthesis. Am J Physiol 266: E829–E839.

Nakatsubo N, Kojima H, Kikuchi K, Nagoshi H, Hirata Y, Maeda D *et al*. (1998). Direct evidence of nitric oxide production from bovine aortic endothelial cells using new fluorescence indicators: diaminofluoresceins. FEBS Lett 427: 263–266.

Ommen SR, Odell JA, Stanton MS (1997). Atrial arrhythmias after cardiothoracic surgery. N Engl J Med 336: 1429–1434.

Radi R (2004). Nitric oxide, oxidants, and protein tyrosine nitration. Proc Natl Acad Sci U S A 101: 4003–4008.

Reinelt P, Karth GD, Geppert A, Heinz G (2001). Incidence and type of cardiac arrhythmias in critically ill patients: a single center experience in a medical-cardiological ICU. Intensive Care Med 17: 1466–1473.

Ross GR, Kang M, Shirwany N, Malykhina AP, Drozd M, Akbarali HI (2007). Nitrotyrosylation of Ca^{2+} channels prevents c-src kinase regulation of colonic smooth muscle contractility in experimental colitis. J Pharmacol Exp Ther 322: 948–956.

Sanguinetti MC (2010). HERG1 channelpathies. Pflugers Arch 460: 265–276.

Skasa M, Jüngling E, Picht E, Schöndube F, Lückhoff A (2001). L-type calcium currents in atrial myocytes from patients with persistent and non-persistent atrial fibrillation. Basic Res Cardiol 96: 151–159.

Tamargo J, Caballero R, Gómez R, Delpón E (2010). Cardiac electrophysiological effects of nitric oxide. Cardiovasc Res 87: 593–600.

Titheradge MA (1999). Nitric oxide in septic shock. Biochim Biophys Acta 1411: 437–455.

Van Wagoner DR (2008). Oxidative stress and inflammation in atrial fibrillation: role in pathogenesis and potential as a therapeutic target. J Cardiovasc Pharmacol 52: 306–313.

Walker D, De Waard M (1998). Subunit interaction sites in voltage-dependent Ca^{2+} channels: role in channel function. Trends Neurosci 21: 148–154.

Zhang Z, He Y, Tuteja D, Xu D, Timofeyev V, Zhang Q *et al*. (2005). Functional roles of $Ca_v1.3$ (α_{1D}) calcium channels in atria insights gained from gene-targeted null mutant mice. Circulation 112: 1936–1944.

Zhong J, Hwang T-C, Adams HR, Rubin LJ (1997). Reduced L-type calcium current in ventricular myocytes from endotoxemic guinea pigs. Am J Physiol 273: H2312–H2324.